Treatment of post-traumatic joint contracture in a rabbit model using pulsed, high intensity laser and ultrasound

Treatment of post-traumatic joint contracture in a rabbit model using pulsed, high intensity laser and ultrasound

David Hazlewood[1], Yi Feng[2], Qinghua Lu[2], Jinxi Wang[2], Xinmai Yang[1,3]

[1]Bioengineering Program and Institute for Bioengineering Research, University of Kansas, Lawrence, KS, USA

[2]Department of Orthopedic Surgery, University of Kansas School of Medicine, Kansas City, KS, USA

[3]Department of Mechanical Engineering, University of Kansas, Lawrence, KS, USA

Correspondence to: Xinmai Yang, PhD, Department of Mechanical Engineering, University of Kansas, Lawrence, KS, 66045

Tel: 785-864-1753; Fax: 785-864-1744; Email: xmyang@ku.edu

Abstract

Post-traumatic joint contracture induced by scar tissues following a surgery or injury can leave patients in a permanent state of pain and disability, which is difficult to resolve by current treatments. This randomized controlled trial examines the therapeutic effect of pulsed high-intensity laser (PHIL) and pulsed high-intensity focused ultrasound (PHIFU) for post-traumatic joint contracture due to arthrofibrosis. The peak power levels of both PHIL and PHIFU are much higher than that of laser or ultrasound currently used in physical therapy, while short pulses are utilized to prevent damage. To test the effectiveness of these treatments, a rabbit knee model for joint contracture was established. 21 rabbits were split into four groups: untreated control (n=5), PHIL (n = 5), PHIFU (n = 5), and a PHIL + PHIFU group (n = 6). Maximum extension of the surgically modified rabbit knee was compared to that of the contralateral control knee over the course of 16 weeks. The rabbits in the untreated control group maintained a relatively consistent level of joint contracture, while every rabbit in each of the treatment groups had improved range of motion, eventually leading to a restoration of normal joint extension. Average recovery time was 7.6 ± 1.5 weeks for the PHIL treatment group, 9.8 ± 3.7 weeks for the PHIFU group, and 8.0 ± 2.2 weeks for the combined treatment group. Histopathology demonstrated reduced density and accelerated resorption of scar tissues in the treated knee joints. This study provides evidence that both PHIL and PHIFU are effective in treating post-traumatic joint contracture in rabbits and warrant further investigation into the underlying mechanisms to optimize PHIL and PHIFU based treatments in a larger number of animals.

Keywords: post-traumatic joint contracture, scar, rabbit model, knee joint, joint capsule, joint immobilization, pulsed high intensity ultrasound, pulsed high intensity laser, arthrofibrosis

Introduction

Patients who can no longer fully extend a joint after it has been injured are considered to have post–traumatic joint contracture, a condition which results in pain, stiffness, and disability for the patient. Post-traumatic joint contracture is often caused by arthrofibrosis, which is defined as a buildup of fibrous scar tissues in the joint, causing a painful reduction in range of motion (ROM) (Petsche and Hutchinson, 1999, Shelbourne and Patel, 1999). Post-traumatic contracture can result from either an initial injury to the joint or as a complication from surgery on the joint, such as anterior cruciate ligament (ACL) reconstruction or total knee arthroscopy (TKA) (Cosgarea et al., 1994). Currently when patients have joint contracture due to arthrofibrosis they will receive either conservative treatment or in more severe cases, surgery to release the contracture, however a complete recovery is not always attained (Enad, 2014, Hutchinson et al., 2005, Schiavone Panni et al., 2009, Schwarzkopf et al., 2013, Kucera et al., 2007, Cosgarea et al., 1994).

Conservative treatment usually includes anti-inflammatory medication, stretching, joint mobilization, strengthening exercises, or therapeutic modalities (i.e. ultrasound or laser) to increase the limited ROM in the joint (Shelbourne and Patel, 1999). To achieve meaningful results, the conservative treatment often requires the aggressive use of physiotherapy (Cheuy et al., 2017). Extensive physical therapy can be very uncomfortable and painful for the patient, which can reduce patient compliance to maintain their exercise and treatment plan.

Patients with more severe joint contracture, or who have been unsuccessful with conservative treatments are referred to surgical intervention. While surgery can be successful for some patients, others may never fully recover normal ROM (Kucera et al., 2007). In some cases the surgery itself may produce scar tissue in and around the joint, resulting in increased joint contracture (Mitsuyasu et al., 2011).

We have developed a combined laser and ultrasound treatment system to reduce post-traumatic joint contracture due to arthrofibrosis. Our treatment system utilizes pulsed high-intensity laser (PHIL) and pulsed high-intensity focused ultrasound (PHIFU.) PHIL and PHIFU can be used independently or can be applied synchronously.

PHIL differs from traditional laser therapies by using high intensity pulses with durations of only a few nanoseconds. For example, the peak intensity of PHIL used in the current study is greater than 10 MW/cm^2; the pulse duration is, however, only 5 ns. These very short pulses cause the photomechanical effect in optically absorbent tissues (McDonald and Wetsel, 1978), such as fresh scar tissue containing high concentrations of hemoglobin. The photomechanical effect creates a stress wave induced by the thermal expansion and contraction after the rapid heating and cooling caused by the short laser pulse. The short pulse duration also prevents the burns and thermal ablation seen in laser resurfacing treatments (Tanzi and Alster, 2002). Laser light has been shown to stimulate cells to promote healing responses through low-level laser therapy (LLLT) (Medrado et al., 2003, Karu, 1987) The higher intensity utilized in PHIL is intended to promote healing in deeper tissues than those targeted in LLLT (Karabut et al., 2016).

Ultrasound has been used to some success in the treatment of post-traumatic joint contracture and musculoskeletal disorders (Tsumaki et al., 2004, Usuba et al., 2006, Naito et al., 2010, Loyola-Sanchez et al., 2012), however the studies investigating its effectiveness mainly utilized low-intensity ultrasound (LIUS) and produced inconsistent results (van der Windt et al., 1999). The applications of high intensity focused ultrasound (HIFU) are not as common in the treatment of musculoskeletal disorders. A limited number of studies showed that HIFU could reduce musculoskeletal pain (Masciocchi et al., 2014, Brown et al., 2015).

PHIFU has been used to disrupt the dense fibrous tissue in a porcine tendons and ligaments of the ankle (Kuo, 2010). Further investigation showed that the tissue was mechanically disrupted and the young's modulus of the tissue was reduced (Yeh et al., 2013). Both of these studies were performed *ex vivo*. The effectiveness of PHIFU on loosening fibrous tissue or relieving joint contracture has not been studied *in vivo*.

When pulsed laser and ultrasound are combined they cause synergistic increase in cavitation (Cui et al., 2013). This phenomenon has been utilized in photo-mediated ultrasound therapy (PUT) to selectively target microvasculature (Hu et al., 2017). In a similar fashion, we will apply both PHIL and PHIFU at the same time to selectively cause cavitation in the scar tissue. The cavitation is intended to provide an additional method of disrupting the collagen fibers of the scar tissue. To treat the dense tissues within the knee higher intensities of both laser and ultrasound will be used in this study compared to those used to target microvessels. The treatment probe was constantly scanned over the treatment area to avoid severe cavitation damage to a particular location.

We studied the effect of ultrasound on relieving joint contracture on a rabbit post-traumatic joint contracture model. Our ultrasound system utilizes high intensity focused ultrasound (HIFU), as opposed the unfocused lower intensity ultrasound that has been utilized. The peak intensity of PHIFU burst employed in the current study is more than 2000 W/cm^2. HIFU creates strong ultrasound intensity at the focal point of a HIFU transducer, while having a weaker intensity near the surface of the tissue. As a result, high dosage of ultrasound energy can be delivered to the focal point, while damage to the surrounding tissues can be avoided. A small duty cycle of 1.5% was used to prevent excessive heating.

Focused ultrasound has been shown to be effective in the treatment of neural tissues in the brain. Higher intensities of ultrasound have been used for direct ablation of neural tissues (Hynynen),

while lower intensities have been used for non-ablative stimulation (Tufail et al., 2011, Lewis et al., 2016). Tyler (Tyler, 2011) proposed that non-ablative stimulation can effectively stimulate the conduction of neurons by increasing membrane permeability through mechanical effects. While the peak intensities of PHIL and PHIFU are comparable to ablative therapies, the short pulses are expected to prevent ablation while causing mechanical effects commonly seen in non-ablative applications. The mechanical effects created by PHIL and PHIFU are expected to cause stimulation of the nerves in the targeted joint, leading to increased muscle activity.

The current study will investigate the independent effect of PHIL and PHIFU, as well as the effect when both techniques are combined. The purpose of both techniques is to create mechanical effects from laser or ultrasound stimulation while avoiding ablation and thermal effects. The peak power levels used in the current study are much stronger than the laser and ultrasound levels traditionally used in physical therapy for musculoskeletal disorders. The short pulses and low duty cycles in the proposed therapies are intended to counteract the increased peak intensity, allowing these high intensity therapies to be used outside of surgical applications. Therefore, the current treatment scheme may open up a new avenue on how to use laser and ultrasound in relieving joint contractures.

Methods and materials

System

The treatment system (figure 1(a)) involved a 532 nm laser (Surelight SLI-30, Continuum, Santa Clara, CA)) system delivering light through an optic fiber to the treatment probe. The laser additionally triggered a function generator (33250A, Agilent Technologies, Santa Clara, CA.) The function generator was connected to a 50 dB power amplifier (350L RF Power Amplifier, ENI

Technology Inc., Rochester, NY) which was then connected to a spherically focused HIFU transducer (H102, Sonic Concepts, Bothell, WA) through a 50-ohm impedance matching circuit.

The treatment probe (figures 1(b) and 1(d)) aligned the 1-MHz transducer with the optical fiber through a central hole in the transducer. The fiber and the transducer were incased in a custom 3D printed cone to help focus the ultrasound waves and hold degassed and deionized water. Water was used for ultrasound transmission. Alignment of the laser fiber was maintained through the use of an additional 3D printed component that attached to the focusing cone. Finally a clear plastic membrane covered the distal end of the cone to prevent water leakage while allowing the laser and ultrasound to transmit effectively.

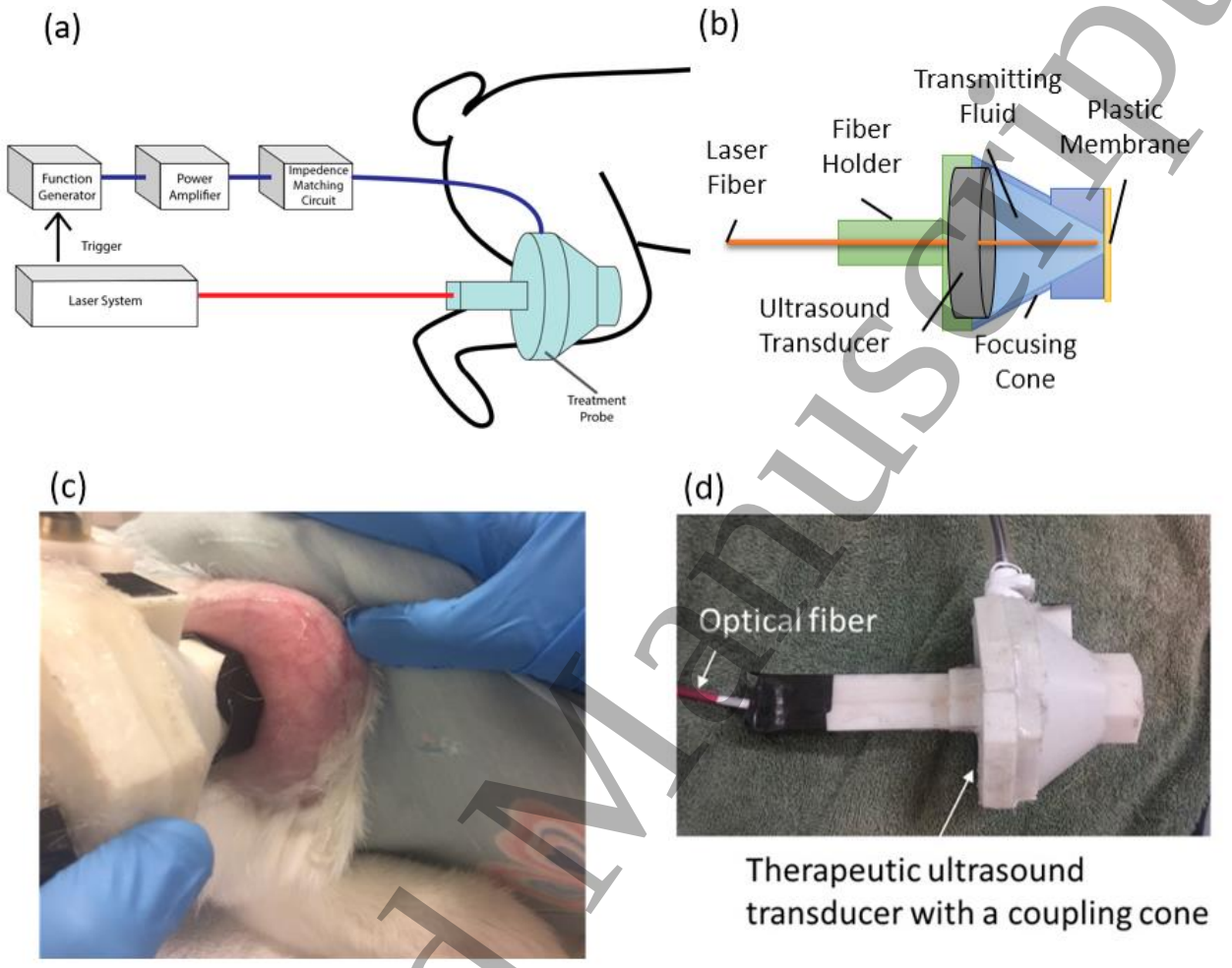

Figure 1. (a) A diagram of the treatment system. (b) A schematic of the treatment probe. (c) A photagraph of treatment probe during use. (d) A photograph of the actual treatment probe.

The ultrasound transducer was used to deliver 1000 cycles of 1-MHz ultrasound when triggered by the laser, creating a 1-ms burst. The 532 nm laser pulse had a 30-Hz repetition rate and a 5-ns pulse duration. The use of the optical fiber limited the maximum laser surface fluence that could be delivered to 52 mJ/cm² in our system. Due to the differences in travel speed, the ultrasound burst must begin before the laser pulse in order for both to arrive at the same time. When the laser triggered the function generator a 33.0-ms delay was added so that the ultrasound burst would

begin just before the next laser pulse. The function generator used in this experiment was unable to detect an incoming trigger while creating an ultrasound burst. This resulted in the PHIFU bursts occurring at a 15-Hz repetition rate, with each PHIFU burst synchronized with every other PHIL pulse. The synchronization between PHIL pulses and PHIFU bursts is shown in Figure 2. An oscilloscope (DPO 3034, Tektronix, Beaverton, OR) was used to confirm that the laser pulse arrived during the beginning of the ultrasound burst.

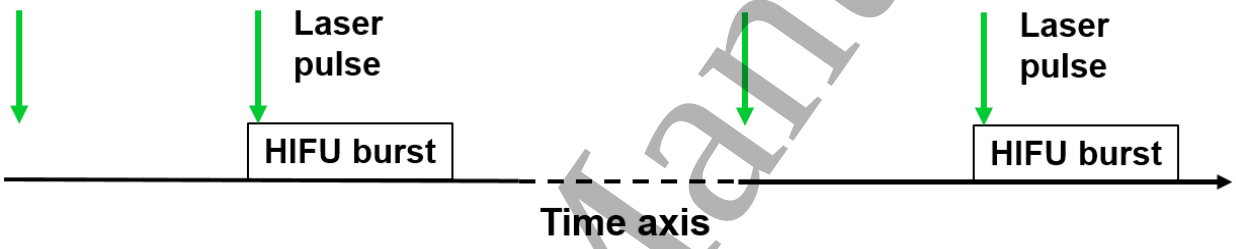

Figure 2. A diagram showing the synchronization of combined PHIL and PHIFU therapies. The HIFU burst is triggered by the laser pulse, however due to differences in travel time a delay is added to insure that the next laser pulse is within the HIFU burst. The Laser pulse arrives at a frequency of 30 Hz. The HIFU burst lasts 1 ms and starts with a frequency of 15 Hz.

In order to select appropriate PHIFU treatment parameters, testing was performed on fresh *ex vivo* rabbit thighs muscles. Cavitation thresholds using PHIFU only were determined through the use of a flat transducer (V310, Olympus Scientific Solutions Technologies Inc., Waltham, MA) as a passive cavitation detector (Madanshetty et al., 1991). A ultrasound burst length of 1 ms with a peak negative pressure of 8 MPa was found to be just below the cavitation threshold. These values

were selected to cause mechanical effects without causing cavitation in PHIFU alone. When both PHIL and PHIFU are combined cavitation was detected in the ex vivo thigh.

A standard calibrated needle hydrophone (0.5 mm Needle hydrophone SN 1462, Precision Acoustics, Dorchester, UK) on a 3D translational stage was used to determine the distribution of the ultrasound emitted from the treatment probe while both were fully submerged in a tank of degassed water. The peak negative pressure of the ultrasound was measured along the central axis for the first 20 mm outside of the treatment probe, and radially at the focal point. The focal point was found to be 6 mm from the treatment probe with a width of 3.2 mm. The hydrophone was only used at pressures under 1 MPa. These results were extrapolated using a finite-difference time-domain (FDTD) simulation as described by Hallaj and Cleveland (Hallaj and Cleveland, 1999), and experimentally validated by Huang et. al. (Huang et al., 2004). Propagation of the ultrasound waves were simulated while accounting for nonlinear effects, acoustic absorption, and the acoustic properties of soft tissue. The simulation required the surface pressure of the transducer during a pulse. The relationship between input voltage and surface pressure of the transducer was determined by comparing hydrophone measurements with simulated results during linear conditions.

Animal Model

We have established a novel knee arthrofibrosis model based on New Zealand rabbit (Hazlewood et al., 2018). New Zealand white rabbits were selected for the animal model due to the relatively large size of their knees. The rabbits were of mixed genders, and aged 6-8 months weighing between 2.8 and 3.6 kg at the time of surgery. Post traumatic joint contracture was created in the right knee of each rabbit through a single surgery. The rabbits were anesthetized through inhalational general anesthesia with isoflurane (to effect) after being sedated with ketamine (40 mg/kg) and xylazine (5 mg/kg). Animals were prepared and draped in the usual sterile fashion

and placed in the supine position. A 15-blade scalpel was used to make a 3.5-cm longitudinal skin incision along the medial collateral ligament and the lateral collateral ligament of the right knee. The lateral 1/3 (posterior to LCL) and the medial 1/3 (posterior to MCL) of the posterior synovium/capsule were transversely incised superficially and then completely disrupted by forceps. The middle 1/3 was partially disrupted by forceps.

In order to facilitate the scar formation in the posterior areas of the knee, a muscle flap was dissected out from the distal portion of biceps femoris, pulled towards the lateral side of upper tibia, and sutured with the superficial layer of the lateral head of gastrocnemius to hold the knee in a flexion position of approximately 60°. This procedure prevented the knee joint from extension (see figures 2(c) and 2(d)). The flexed immobilization was further enhanced by pulling the superficial layer of the medial flexors together with absorbable sutures (4-0 Vicryl, Ethicon). The deep fascia was closed with absorbable sutures (4-0 Vicryl, Ethicon). The skin incisions were then closed with 4-0 non-absorbable sutures. E-collars were placed around the necks of the rabbits as they recovered from anesthesia. The non-operated left knee was used as a baseline control. After surgery, animals were allowed free cage activity. The operated rabbits were monitored for pain and received meloxicam (0.2 g/kg) as an analgesic as determined by the monitoring veterinarian.

Post-operative measurements

During the 8-week recovery period the operated knee was not immobilized, and the rabbits were allowed to use the leg as desired. This experimental design was chosen for multiple reasons. Firstly, by not immobilizing the knee it prevented knee contracture that might be due to the immobilization of the knee. Secondly, this reduced the amount of muscle atrophy in the musculature knee. Some atrophy is to be expected with arthrofibrosis of the knee, but additional

atrophy would have been caused if the knee had been immobilized. Finally, allowing the rabbits to use the operated leg as desired dramatically reduced the stress in the rabbits.

A training program was also performed during the 8-week recovery period. The rabbits were wrapped in a towel and held by a researcher for increasing periods of time up to 20 minutes. At the end of this time the rabbit was rewarded with a small piece of fruit and returned to its cage. The goal of the training program was to acclimate the rabbits to being held in order to reduce stress and movement during later treatments and measurements of knee flexion contracture.

Starting eight weeks after the surgery, weekly measurements were performed to determine the severity of knee contracture. For the health of the rabbits they were not anaesthetized during these measurements. The rabbit was first wrapped in a towel and gently held in a position where it was laying on its side. The leg was exposed and the thigh was held against the body in a natural crouched position. The angle between the longitudinal axis of the femur and tibia were measured, with the center of the patella placed at the vertex of the angle. A strap was placed around the leg 10 cm from the knee. A force of 2 N was applied to extend the knee joint. The force was verified by a spring force gauge. The resulting torque of 0.2 N•m (or 20 N•cm) was the same as used in previous studies (Barlow et al., 2013, Nesterenko et al., 2009). Other studies have used a torque of 0.49 N•m (Fukui et al., 2001, Fukui et al., 2000), however the lower value was selected to prevent any therapeutic effect from the additional stretching. Cares were taken to ensure that the rabbit was not resisting or forcing the leg during the measurement. The extension angle from the 0.2 N•m torque between the femur and the tibia was measured. Net flexion contracture was calculated by taking the difference in maximum extension between the operated knee and contralateral control knee. Five repeated measurements throughout the course of a day were used to estimate the measurement error of 3°.

Treatment

Rabbits were randomly placed into one of four treatment groups. The first group received PHIL treatment. The PHIL group received 532 nm laser light with a surface fluence of 52 mJ/cm² at 30 Hz of 5-ns laser pulses (corresponding to ~10.4 MW/cm^2 peak intensity). The second group received PHIFU treatment. The PHIFU group received 1000 sine wave cycles of 1 MHz ultrasound with a peak negative pressure of 8 MPa (corresponding to ~2133 W/cm^2 peak intensity). The third group received combined PHIL and PHIFU treatment simultaneously. Finally a fourth group was used as a control without treatment. The combined group received both treatments at the same time, with every other laser pulse synchronized with the ultrasound burst (figure 2).

Treatments were performed twice weekly. During each treatment, the rabbits were placed into a soft restraint cloth first. The restraint cloth covered the rabbit in soft material while providing a slit for the operated knee to be exposed. The restraint cloth also covered the eyes of the rabbits to prevent possible laser exposure. The knee was shaved with an electric razor to expose skin. A treatment area with a diameter of approximately 5 cm was selected on the lateral side of the leg slightly posterior to the tibial plateau. EMLA cream was applied to the treatment area for proactive pain relief. Ultrasound coupling gel was applied to the knee to insure acoustic transmission. Each treatment session lasted for 10 minutes. During this time the treatment probe was gently moved across the treatment area to prevent skin damage or irritation from prolonged treatment at a single location. Afterwards the ultrasound gel was wiped from the knee, and the rabbit was returned to its cage.

During the course of our treatment the rabbits very occasionally showed signs of distress, however in every case that this happened it appeared to be from the rabbit resisting the restraint as opposed

to a response to the actual treatment. If needed the treatment would be paused until the rabbit was calmed. These breaks took no longer than one minute.

Histology and Histochemistry

At the designated endpoints, rabbits were euthanized by the injection of 1 ml of commercial available euthanasia solution containing pentobarbital (Vortech Pharmaceuticals, Dearborn, MI). Upon euthanasia, both the operated and non-operated knee joints were harvested. The harvested knee joints were fixed in 10% buffered formalin (American MasterTech, Lodi, CA) for 7-10 days, then decalcified in 25% formic acid (Sigma, St. Louis, MO), and embedded in paraffin (Leica Biosystems, Richmond, IL). The samples were then sectioned at 5 μm, and stained with hematoxylin and eosin (H&E) to observe the general tissue structures. Safranin O and fast green stains were used to identify cartilage cells and matrices as described previously (Xu et al., 2007, Wang et al., 2009, Rodova et al., 2011, Wang, 2000). In order to identify the spatial relationship between the joint structure and scar tissues, the knee joint samples were sectioned in either cross or sagittal orientation.

Statistical Analysis

The resulting measurements of flexion contracture are presented as means ± standard deviation. The various means were then compared using Student's t-Test (two-sample, two-tailed, unequal variance). Fisher's exact test was used to compare the recovery rates of the different groups. The null hypothesis was that there was no effect from the treatment regime compared to the control. Statistical significance for all studies was $p < 0.05$.

Results

Flexion Contracture Measurement

Twenty-one rabbits were used in this study with 5 being used in the untreated control, PHIL, and PHIFU group, while 6 rabbits were used in the combined group. Weekly averages of net flexion contracture measurements for each group are summarized in Table 1. Statistical significance was determined through the use of Student's t-Test by comparing each treatment group with the control group for each week of measurements. Once a rabbit reached a complete recovery, defined as maximal knee extension in both knees within measurement error, it was euthanized and considered to have a net flexion contracture of 0 degrees for all further weeks. Figure 3 shows the average time required for each group to make a complete recovery.

It can be seen that all three of the treatment groups eventually showed statistically significant improvement when compared to the control group. Additionally, all of the rabbits that received treatment made a complete recovery, while no subjects in the control group made a complete recovery within the 16 weeks of the study ($p = 0.008$). The average period of time required for complete recovery was 7.6 ± 1.5 weeks for the PHIL treated group, 9.8 ± 3.7 weeks for the PHIFU treated group, and 8.0 ± 2.2 weeks for the combined treatment group. However, the differences in average recovery time between all treatment groups were not statistically significant with the number of rabbits used in this study. One rabbit in the PHIFU treatment group was found to have additional bone growth in the treated knee, and also had the slowest recovery. However, the differences in average recovery time between all treatment groups were not statistically significant.

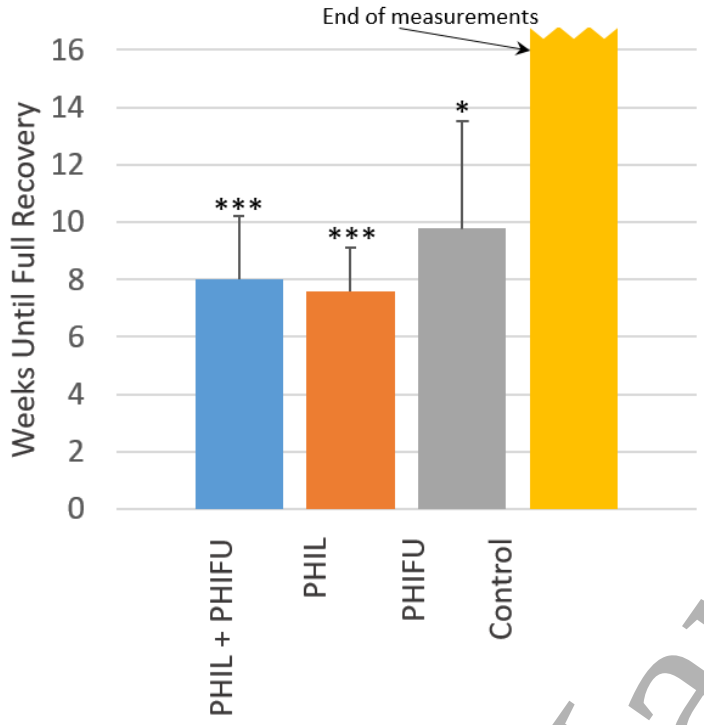

Figure 3. A plot demonstrating the number of weeks required until complete recovery for each of the treated rabbits. No subjects in the control group made a complete recovery before the end of the study (16 weeks), while all of the treated rabbits regained normal range of motion. For statistical comparisons the control group was treated as recovering during week 16, however based on the relatively steady level of contracture it is most likely that the control subjects would have never regained normal range of motion. * represents $p < 0.05$ when compared to the control group. *** represents $p < 0.001$ when compared to the control group.

Table 1: Flexion contracture measurements were taken by measuring the angle of extension when a 0.2 Nm torque was applied to extend the knee. The presented results represent the difference between the model knee and the contralateral control knee. Measurements were performed weekly for 16 weeks or until there was equivalent flexion contracture in both knees. p-values were determined through comparisons to the control group. "*" represents weeks when all of the subjects in the given group had made a full recovery.

Week Post-Surgery	Control (N = 5)	PHIL (N=5)	PHIFU (N = 5)	Combined (N = 6)
8	22 ± 5.7	21.8 ± 5.4 (p = 0.956)	22.4 ± 4.9 (p = 0.908)	21.7 ± 6.8 (p = 0.932)
9	17.8 ± 2.6	20.6 ± 4.3 (p = 0.258)	22.8 ± 5.6 (p = 0.125)	16.7 ± 4.6 (p = 0.623)
10	24.4 ± 6.7	16.2 ± 5.5 (p = 0.068)	17.8 ± 6.7 (p = 0.156)	16.5 ± 5.2 (p = 0.065)
11	21.2 ± 6.2	17.8 ± 7 (p = 0.439)	18.4 ± 7.3 (p = 0.53)	13.7 ± 5.2 (p = 0.063)
12	20 ± 7.1	11.8 ± 4.6 (p = 0.067)	12.6 ± 7.2 (p = 0.139)	13.5 ± 6 (p = 0.142)
13	22.6 ± 4.3	10.6 ± 7.9 (p = 0.024)	13.2 ± 7.9 (p = 0.056)	10.2 ± 5.7 (p = 0.003)
14	17.4 ± 5.3	9.6 ± 8.4 (p = 0.122)	6.8 ± 4.4 (p = 0.009)	9.8 ± 7 (p = 0.071)
15	16.4 ± 4.2	4.6 ± 3.2 (p = 0.001)	7.4 ± 4.9 (p = 0.014)	4.5 ± 5.7 (p = 0.003)
16	19.2 ± 8.1	2.4 ± 4.8 (p = 0.006)	7 ± 4.5 (p = 0.025)	3.3 ± 5.3 (p = 0.008)
17	21.2 ± 4.8	*	4.2 ± 4.4 (p < 0.001)	3.5 ± 6.4 (p = 0.001)
18	18 ± 6.3	*	2.8 ± 2.8 (p = 0.003)	1 ± 3 (p = 0.002)
19	18.4 ± 4.7	*	2.4 ± 7.2 (p = 0.004)	*
20	14.6 ± 5.7	*	2 ± 4.5 (p = 0.005)	*
21	16.6 ± 2.3	*	1 ± 2.2 (p < 0.001)	*
22	17 ± 7.7	*	2 ± 4.5 (p = 0.008)	*
23	18.4 ± 7.8	*	*	*
24	17.8 ± 8	*	*	*

Histological Analysis

Experimental rabbits were euthanized for histological analyses of the knee joints at 24 weeks post-surgery. Tissue sections were microscopically examined through both conventional and polarizing lenses, with a main focus on the posterior region of the knee joints where the joint capsule was disrupted in the operated animals. In the non-operated knees, the normal joint capsules displayed intact fibrous structure with well-organized collagen orientation when viewed under polarizing lenses (figures 4(A) and 4(B)). The untreated group demonstrated disorganized, dense scar formation in the area with capsule disruption with little evidence of scar tissue resorption (figures 4(C) and 4(D)). The treated groups receiving PHIL, PHIFU, or PHIL plus PHIFU showed similar histopathological changes, characterized by less dense scar tissue with active capillary formation and vascular invasion, indicating the resorption of scar tissues. The representative micrographs taken from the PHIL plus PHIFU group are presented in figures 4(E) and 4(F). No burnt or necrotic tissues were observed in or around the joint, suggesting that the therapeutic methods used in this study are safe with no obvious tissue damage.

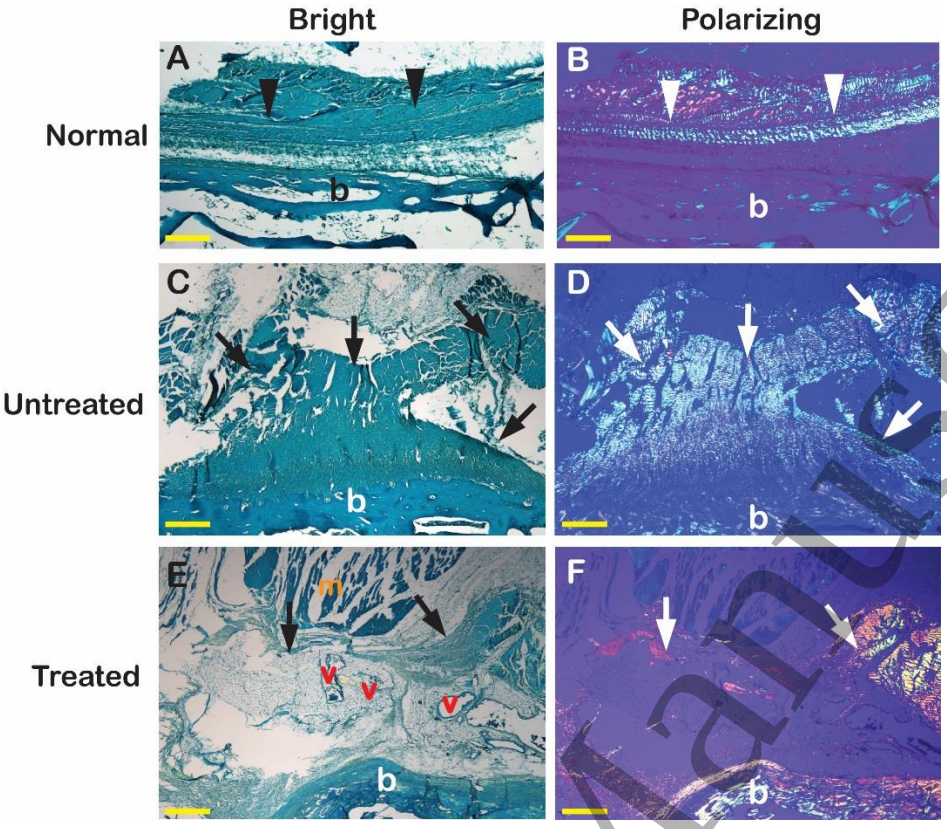

Figure 4. Micrographs of normal knee joint capsule (Normal), disrupted capsule without treatment (Untreated), and disrupted capsule with PHIFU plus PHIL therapy (Treated) at 24 weeks after posterior capsule disruption of rabbit knees. **(A) and (B)**: Normal knee joint capsule in the posterior region of a non-operated knee. **(C) and (D):** An untreated knee with capsule damage showing dense scar formation in the posterior region of the joint. **(E) and (F):** A knee joint with capsule damage treated by a combination of PHIFU and PHIL showing less dense scar tissue with capillary formation (v). Arrowheads: normal joint capsule. b: bone tissue adjacent to the joint margin. Arrows: scar tissue formed in the disrupted capsule regions. v: newly formed capillaries or blood vessels in scar tissue. m: muscles. Safranin-O and fast green stains. Scale bar = 200 μm.

Discussion

All three of the tested treatment groups showed a statistically significant improvement when compared to the untreated control, demonstrating that these modalities may be effective in the treatment of knee flexion contracture caused by arthrofibrosis. This conclusion was shown through weekly measurements of flexion contracture, as well as through histological analysis.

One rabbit in PHIFU group was found to have additional bone growth in the treated knee. This caused the joint to become wider than the contralateral control knee. This rabbit also had the longest recovery time of all of the treated subjects. The cause of this complication is unclear. It would be possible that prolonged PHIFU therapy caused pathological bone growth, or surgical damage to the joint capsule resulted in osteophyte formation. More investigation into this matter is warranted.

While all three treatments were effective, the differences in recovery times were not statistically significant when compared between treatment groups. We hypothesized that if both PHIL and PHIFU were successful, then the combined treatment would have even greater success, however all three treatment groups had similar results. The most likely cause is the large uncertainty in this study. The number of animals in this study was selected to determine if the treatments were effective compared to the control group. Additional studies with larger numbers of test subjects are needed to determine if there are statistically significant differences between the different treatment methods. Power analysis suggests that minimum groups of n = 25 are needed to compare the recovery times of PHIFU and PHIL groups.

The mechanism of action for PHIFU and PHIL treatment is not exactly clear. One of the possible mechanisms is the biomechanical stimulation induced by the ultrasound and laser. The high

intensity used in PHIFU can produce mechanical effects such as acoustic radiation force (ARF) that may stimulate the tissue (ter Haar, 2007). These forces may cause a vibration at the pulse repetition rate similar to those used in vibrational therapy (Mano et al., 2015). PHIL utilizes high-peak-intensity laser with short pulse duration, typically less than 10 ns. As a result, PHIL can induce strong acoustic pulses through the photoacoustic (PA) effect in any tissue that has strong optical absorption at the peak intensity employed in the current study (Jo and Yang, 2016). The strong PA pulse may serve as a secondary source of vibratory stimuli on tissue, particularly for strongly optically absorptive tissue, such as fresh scars that contain high concentrations of hemoglobin.

The other possible mechanism is mechanical separation of the scar tissue, or cavitation. This may be achieved directly through the large rarefaction pressures to induce micro cavitation in the scar tissue. Because of the employed high intensity of laser and ultrasound, micro cavitation may be induced in fibrous tissues and cause micro lesions, resulting in the remodeling of the fibrous tissues and relief of the contracture.

Whenever high intensity laser and ultrasound are used, safety would be a concern. The laser fluence level used in the current study (52 mJ/cm^2) is greater than the laser safety limit for human skin exposure (20 mJ/cm^2) (2007). However, we did not observe any burnt or necrotic tissues either on the skin or inside the treated rabbit knees. In addition, our HIFU burst is only 1-ms, which is faster than a single action potential. This is expected to lead to reduced perception of the burst in a similar fashion as seen is very short audio pulses (Everest, 2001). As a result rabbits did not show any resistance to the treatment, indicating that the treatment is safe and tolerable.

It should be noted that while it has been demonstrated that PHIL can successfully treat arthrofibrosis in rabbit knee joints, it is expected to have a reduced effect in human joints. The

limited penetration depth of laser therapies is expected limit effective treatment of scars to those within one centimeter of the skin surface. Laser based therapies have an advantage over ultrasound based therapies by selectively targeting optically absorbent tissues. The limited penetration, and the selective targeting suggests that PHIL may be best suited to the treatment of smaller joints, or the parts of larger joints that are close to the surface. While PHIFU is more difficult to target, it is able to achieve much greater penetration depths, suggesting that it holds great promise in the treatment of arthrofibrosis in shoulders, knees, and other larger joints.

Future work intends to refine the treatment parameters, such as duration and intensity, to optimize the treatment. An addition goal is to determine if these therapies can be applied during the initial recovery from an injury or surgery to prevent post traumatic joint contracture.

In conclusion this study has shown important proof of concept success for PHIL and PHIFU therapies. Both methods as well as a combined treatment resulted in statistically significant improvement when compared to the untreated control group. This was shown through measurement of knee flexion contracture and histological analysis. All of the rabbits that received one of the treatments achieved a complete recovery, with a normal range of knee extension that was the same as that of the contralateral control knee. The rabbits in the untreated control group were unable to achieve a complete recovery and maintained a consistent level of flexion contracture.

Author Contributions Statement

J Wang, D. Hazlewood, and X. Yang: Substantial contribution to the design and conduct of animal experiment, the acquisition and interpretation of data, and manuscript preparation. Y Feng and Q

Lu: Substantial contribution to the acquisition of data and manuscript preparation. All authors have read and approved the final submitted manuscript.

ACKNOWLEDGMENTS

This work was supported by a medical research grant from the United States Department of Defense (DoD) under Award Number W81XWH-15-1-0524. The authors thank Dr. Da Zhang (Professor of Pathology at the University of Kansas Medical Center) for his histopathological analysis of rabbit knee joints. The authors have no conflict of interest to declare.

References

American National Standard for Safe Use of Lasers ANSI Z136.1-2007. Orlando, FL: Laser Institute of America, American National Standards Institute.

BARLOW, J. D., HARTZLER, R. U., ABDEL, M. P., MORREY, M. E., AN, K. N., STEINMANN, S. P., MORREY, B. F. & SANCHEZ-SOTELO, J. 2013. Surgical capsular release reduces flexion contracture in a rabbit model of arthrofibrosis. *J Orthop Res,* 31**,** 1529-32.

BROWN, M. R. D., FARQUHAR-SMITH, P., WILLIAMS, J. E., TER HAAR, G. & DESOUZA, N. M. 2015. The use of high-intensity focused ultrasound as a novel treatment for painful conditions-a description and narrative review of the literature. *British Journal of Anaesthesia,* 115**,** 520-530.

CHEUY, V. A., FORAN, J. R. H., PAXTON, R. J., BADE, M. J., ZENI, J. A. & STEVENS-LAPSLEY, J. E. 2017. Arthrofibrosis Associated With Total Knee Arthroplasty. *Journal of Arthroplasty,* 32**,** 2604-2611.

COSGAREA, A. J., DEHAVEN, K. E. & LOVELOCK, J. E. 1994. THE SURGICAL-TREATMENT OF ARTHROFIBROSIS OF THE KNEE. *American Journal of Sports Medicine,* 22**,** 184-191.

CUI, H. Z., ZHANG, T. & YANG, X. M. 2013. Laser-enhanced cavitation during high intensity focused ultrasound: An in vivo study. *Applied Physics Letters,* 102**,** 4.

ENAD, J. G. 2014. Arthroscopic Lysis of Adhesions for the Stiff Total Knee Arthroplasty. *Arthroscopy Techniques,* 3**,** e611-e614.

EVEREST, F. A. 2001. *The master handbook of acoustics,* New York, McGraw-Hill.

FUKUI, N., NAKAJIMA, K., TASHIRO, T., ODA, H. & NAKAMURA, K. 2001. Neutralization of fibroblast growth factor-2 reduces intraarticular adhesions. *Clinical Orthopaedics and Related Research***,** 250-258.

FUKUI, N., TASHIRO, T., HIRAOKA, H., ODA, H. & NAKAMURA, K. 2000. Adhesion formation can be reduced by the suppression of transforming growth factor-beta 1 activity. *Journal of Orthopaedic Research,* 18**,** 212-219.

HALLAJ, I. M. & CLEVELAND, R. O. 1999. FDTD simulation of finite-amplitude pressure and temperature fields for biomedical ultrasound. *Journal of the Acoustical Society of America,* 105**,** L7-L12.

HAZLEWOOD, D., FENG, Y., LU, Q., YANG, X. & WANG, J. 2018. Novel rabbit model of moderate knee contracture induced by direct capsular damage. *J Orthop Res*.

HU, Z. Z., ZHANG, H. N., MORDOVANAKIS, A., PAULUS, Y. M., LIU, Q. H., WANG, X. D. & YANG, X. M. 2017. High-precision, non-invasive anti-microvascular approach via concurrent ultrasound and laser irradiation. *Scientific Reports,* 7**,** 12.

HUANG, J., HOLT, R. G., CLEVELAND, R. O. & ROY, R. A. 2004. Experimental validation of a tractable numerical model for focused ultrasound heating in flow-through tissue phantoms. *Journal of the Acoustical Society of America,* 116**,** 2451-2458.

HUTCHINSON, J. R. M., PARISH, E. N. & CROSS, M. J. 2005. Results of open arthrolysis for the treatment of stiffness after total knee replacement. *Journal of Bone & Joint Surgery, British Volume,* 87-B**,** 1357-1360.

HYNYNEN, K. Pre-clinical testing of a phased array ultrasound system for MRI-guided noninvasive surgery of the brain—A primate study. *European journal of radiology,* 59**,** 149-156.

JO, J. & YANG, X. 2016. Laser-enhanced high-intensity focused ultrasound heating in an in vivo small animal model. *Applied Physics Letters,* 109**,** 213702.

KARABUT, M. M., GLADKOVA, N. D. & FELDCHTEIN, F. I. 2016. Fractional Laser Photothermolysis in the Treatment of Skin Defects: Possibilities and Effectiveness. *Sovremennye Tehnologii V Medicine,* 8**,** 98-107.

KARU, T. I. 1987. PHOTOBIOLOGICAL FUNDAMENTALS OF LOW-POWER LASER THERAPY. *Ieee Journal of Quantum Electronics,* 23**,** 1703-1717.

KUCERA, T., URBAN, K., KARPAS, K. & SPONER, P. 2007. Restricted motion after total knee arthroplasty. *Acta Chirurgiae Orthopaedicae Et Traumatologiae Cechoslovaca,* 74**,** 326-331.

KUO, P.-L. 2010. Joint capsule loosening by high-intensity pulsed ultrasound. IEEE.

LEWIS, P. M., THOMSON, R. H., ROSENFELD, J. V. & FITZGERALD, P. B. 2016. Brain Neuromodulation Techniques: A Review. *Neuroscientist,* 22**,** 406-421.

LOYOLA-SANCHEZ, A., RICHARDSON, J., BEATTIE, K. A., OTERO-FUENTES, C., ADACHI, J. D. & MACINTYRE, N. J. 2012. Effect of Low-Intensity Pulsed Ultrasound on the Cartilage Repair in People With Mild to Moderate Knee Osteoarthritis: A Double-Blinded, Randomized, Placebo-Controlled Pilot Study. *Archives of Physical Medicine and Rehabilitation,* 93**,** 35-42.

MADANSHETTY, S. I., ROY, R. A. & APFEL, R. E. 1991. ACOUSTIC MICROCAVITATION - ITS ACTIVE AND PASSIVE ACOUSTIC DETECTION. *Journal of the Acoustical Society of America,* 90**,** 1515-1526.

MANO, S., PALINKAS, J., SZABO, J., NAGY, J. T., BAKO, K. & CSERNATONY, Z. 2015. Application of a vibrating device for the prevention of flexion contracture after total knee arthroplasty. *Eur J Orthop Surg Traumatol,* 25**,** 167-72.

MASCIOCCHI, C., CONCHIGLIA, A., GREGORI, L. M., ARRIGONI, F., ZUGARO, L. & BARILE, A. 2014. Critical role of HIFU in musculoskeletal interventions. *Radiologia Medica,* 119**,** 470-475.

MCDONALD, F. A. & WETSEL, G. C. 1978. GENERALIZED THEORY OF PHOTOACOUSTIC EFFECT. *Journal of Applied Physics,* 49**,** 2313-2322.

MEDRADO, A., PUGLIESE, L. S., REIS, S. R. A. & ANDRADE, Z. A. 2003. Influence of low level laser therapy on wound healing and its biological action upon myofibroblasts. *Lasers in Surgery and Medicine,* 32**,** 239-244.

MITSUYASU, H., MATSUDA, S., MIURA, H., OKAZAKI, K., FUKAGAWA, S. & IWAMOTO, Y. 2011. Flexion Contracture Persists If the Contracture is More Than 15 degrees at 3 Months After Total Knee Arthroplasty. *Journal of Arthroplasty,* 26**,** 639-643.

NAITO, K., WATARI, T., MUTA, T., FURUHATA, A., IWASE, H., IGARASHI, M., KUROSAWA, H., NAGAOKA, I. & KANEKO, K. 2010. Low-Intensity Pulsed Ultrasound (LIPUS) Increases the Articular Cartilage Type II Collagen in a Rat Osteoarthritis Model. *Journal of Orthopaedic Research,* 28**,** 361-369.

NESTERENKO, S., MORREY, M. E., ABDEL, M. P., AN, K. N., STEINMANN, S. P., MORREY, B. F. & SANCHEZ-SOTELO, J. 2009. New rabbit knee model of posttraumatic joint contracture: indirect capsular damage induces a severe contracture. *J Orthop Res,* 27**,** 1028-32.

PETSCHE, T. S. & HUTCHINSON, M. R. 1999. Loss of extension after reconstruction of the anterior cruciate ligament. *The Journal of the American Academy of Orthopaedic Surgeons,* 7**,** 119-27.

RODOVA, M., LU, Q., LI, Y., WOODBURY, B. G., CRIST, J. D., GARDNER, B. M., YOST, J. G., ZHONG, X. B., ANDERSON, H. C. & WANG, J. 2011. Nfat1 regulates adult articular chondrocyte function through its age-dependent expression mediated by epigenetic histone methylation. *J Bone Miner Res,* 26**,** 1974-86.

SCHIAVONE PANNI, A., CERCIELLO, S., VASSO, M. & TARTARONE, M. 2009. Stiffness in total knee arthroplasty. *Journal of Orthopaedics and Traumatology : Official Journal of the Italian Society of Orthopaedics and Traumatology,* 10**,** 111-118.

SCHWARZKOPF, R., WILLIAM, A., DEERING, R. M. & FITZ, W. 2013. Arthroscopic lysis of adhesions for stiff total knee arthroplasty. *Orthopedics,* 36**,** e1544-8.

SHELBOURNE, K. D. & PATEL, D. V. 1999. Treatment of limited motion after anterior cruciate ligament reconstruction. *Knee Surgery Sports Traumatology Arthroscopy,* 7**,** 85-92.

TANZI, E. L. & ALSTER, T. S. 2002. Treatment of atrophic facial acne scars with a dual-mode Er : YAG laser. *Dermatologic Surgery,* 28**,** 551-555.

TER HAAR, G. 2007. Therapeutic applications of ultrasound. *Progress in Biophysics & Molecular Biology,* 93**,** 111-129.

TSUMAKI, N., KAKIUCHI, M., SASAKI, J., OCHI, T. & YOSHIKAWA, H. 2004. Low-intensity pulsed ultrasound accelerates maturation of callus in patients treated with opening-wedge high tibial osteotomy by hemicallotasis. *Journal of Bone and Joint Surgery-American Volume,* 86A**,** 2399-2405.

TUFAIL, Y., YOSHIHIRO, A., PATI, S., LI, M. M. & TYLER, W. J. 2011. Ultrasonic neuromodulation by brain stimulation with transcranial ultrasound. *Nature Protocols,* 6**,** 1453-1470.

TYLER, W. J. 2011. Noninvasive Neuromodulation with Ultrasound? A Continuum Mechanics Hypothesis. *Neuroscientist,* 17**,** 25-36.

USUBA, M., MIYANAGA, Y., MIYAKAWA, S., MAESHIMA, T. & SHIRASAKI, Y. 2006. Effect of heat in increasing the range of knee motion after the development of a joint contracture: An experiment with an animal model. *Archives of Physical Medicine and Rehabilitation,* 87**,** 247-253.

VAN DER WINDT, D., VAN DER HEIJDEN, G., VAN DEN BERG, S. G. M., TER RIET, G., DE WINTER, A. F. & BOUTER, L. M. 1999. Ultrasound therapy for musculoskeletal disorders: A systematic review. *Pain,* 81**,** 257-271.

WANG, J. 2000. Spatial orientation of the microscopic elements of cortical repair bone. *Clin Orthop Relat Res***,** 265-77.

WANG, J., GARDNER, B. M., LU, Q., RODOVA, M., WOODBURY, B. G., YOST, J. G., ROBY, K. F., PINSON, D. M., TAWFIK, O. & ANDERSON, H. C. 2009. Transcription factor Nfat1 deficiency causes osteoarthritis through dysfunction of adult articular chondrocytes. *J Pathol,* 219**,** 163-72.

XU, L., ANDERSON, A. L., LU, Q. & WANG, J. 2007. Role of fibrillar structure of collagenous carrier in bone sialoprotein-mediated matrix mineralization and osteoblast differentiation. *Biomaterials,* 28**,** 750-61.

YEH, C. L., LI, P. C., SHIH, W. P., HUANG, P. S. & KUO, P. L. 2013. Imaging monitored loosening of dense fibrous tissues using high-intensity pulsed ultrasound. *Physics in Medicine and Biology,* 58**,** 6779-6796.